degrees of freedom. In the simple version developed here, we have included only R_{AB} and the center-of-mass coordinate r. The center-of-mass motion accepts the energy released in the deactivating vibronic transitions originating from levels i of $(A\cdots B)^*$.

In general, of course, a variety of modes may strongly participate in the dynamics of either relaxation process (see eq 2 and 3). For example, like the COM mode of AB, the orientational mode of AB or the COM (or orientational) modes of the solvent (S) molecules are of relatively low frequency and could function to accept relatively small amounts of energy. Hence, these modes should efficiently mediate relatively low-energy vibronic transitions. On the other hand, the internal vibrational modes of AB or S are of relatively high frequency and could, by single or few-quantum excitations, with the assistance of the lower frequency COM modes, provide many pathways by which higher energy vibronic transitions could be mediated. The efficiency of these various pathways depends, of course, upon the strength of coupling between R_{AB} and the accepting mode.

It is of interest to note the close analogy that exists between the present view of photodissociation processes and the previously described model for the photosynthetic primary light reaction.[25] The photoactivation of $(A\cdots B)^*$ followed by the primary dissociative reaction to yield the A* and B* fragments in the present case corresponds formally to the photoexcitation of the charge transfer (CT) state in the reaction-center chlorophyll {Chl a} resulting in the oxidation of {Chl a} and the reduction of the primary electron acceptor A in the photosynthesis problem (compare Figure 1 with Figure 1 of ref 25). In both cases, the quasi-bound state $(A\cdots B)^*$ and the CT state in {Chl a} are envisaged to be electronically excited states of the *reactants*. Both of these states are photophysically connected with their respective ground-state species through nonreactive pathways with associated rate constants given approximately by eq 9.

We close by emphasizing that our concept of the *reactive complex* differs fundamentally from that of the *activated complex* in transition-state theory. Unlike the activated complex, a transient species located at the top of the barrier to chemical reaction, the reactive complex in our theory is a stable molecular entity (in the zeroth order of time-dependent perturbation theory). Aside from this conceptual difference, the present formulation provides explicit expressions for the rate constant, eq 4 and 9, in terms of molecular parameters and thermodynamic state variables (e.g., temperature). Numerical fits of rate data using eq 4 and 9 should therefore furnish useful information about the microscopic properties of the system which are most influential in determining its dynamical behavior.

References and Notes

(1) F. K. Fong and D. J. Diestler, *J. Chem. Phys.*, **57**, 4953 (1972).
(2) S. H. Lin and H. Eyring, *Proc. Natl. Acad. Sci. U.S.A.*, **69**, 3192 (1972).
(3) K. F. Freed and F. K. Fong, *J. Chem. Phys.*, **63**, 2890 (1975).
(4) F. K. Fong, *J. Am. Chem. Soc.*, **96**, 7638 (1974).
(5) V. M. Fain, *J. Chem. Phys.*, **65**, 1854 (1976).
(6) S. H. Lin, K. P. Li, and H. Eyring, *Phys. Chem.*, **7**, 1 (1975).
(7) F. K. Fong, "Theory of Molecular Relaxation", Wiley-Interscience, New York, N.Y., 1975: (a) Section 5.4; (b) Chapter 6.
(8) F. K. Fong, *Acc. Chem. Res.*, **9**, 433 (1976).
(9) F. K. Fong, *J. Am. Chem. Soc.*, submitted.
(10) H. Eyring, *J. Chem. Phys.*, **3**, 107 (1935).
(11) W. Kauzmann, *Rev. Mod. Phys.*, **14**, 12 (1942).
(12) K. J. Laidler, "Theories of Chemical Reaction Rates", McGraw-Hill, New York, N.Y., 1969.
(13) G. Porter, V. Balzani, and L. Moggi, *Adv. Photochem.*, **9**, 147 (1974).
(14) K. F. Freed in "Topics in Applied Physics", Vol. 15, F. K. Fong, Ed., Springer-Verlag, Heidelberg, 1976, Chapter 2.
(15) D. J. Diestler in ref 14, Chapter 3.
(16) W. M. Gelbart, K. F. Freed, and S. A. Rice, *J. Chem. Phys.*, **52**, 2460 (1970).
(17) A. Warshel and M. Karplus, *Chem. Phys. Lett.*, **32**, 11 (1975).
(18) S. Mukamel and J. Jortner, *J. Chem. Phys.*, **65**, 3735 (1976).
(19) See, for example, D. A. McQuarrie, "Statistical Thermodynamics", Harper and Row, New York, N.Y., 1973, Chapter 12.
(20) K. F. Freed and J. Jortner, *J. Chem. Phys.*, **52**, 6272 (1970).
(21) S. F. Fischer, *J. Chem. Phys.*, **53**, 3195 (1970).
(22) T. J. Chaung, G. W. Hoffman, and K. B. Eisenthal, *Chem. Phys. Lett.*, **25**, 201 (1974).
(23) A. Nitzan and J. Jortner, *J. Chem. Phys.*, **58**, 2412 (1973).
(24) W. A. Wassam and F. K. Fong, *J. Chem. Phys.*, **65**, 3102 (1976).
(25) F. K. Fong, *J. Am. Chem. Soc.*, **98**, 7840 (1976).

Strengths of A–A Single Bonds in Symmetric A2B2n Molecules and Ions[1]

Benjamin M. Gimarc,*[2] Shakil A. Khan, and Michael C. Kohn

Contribution from the Department of Chemistry, University of South Carolina, Columbia, South Carolina 29208. Received March 14, 1977

Abstract: In symmetric A_2B_4 molecules and ions with 34 and 38 valence electrons, two AB_2 monomers are joined by an A–A single bond. In 50-electron ethanelike A_2B_6 structures, two AB_3 monomers are also linked by an A–A single bond. Symmetric BAAB systems with 18 and 26 electrons have A–A single bonds. A qualitative MO model of the electronic structures of these systems is developed and then used to explain observed trends of increasing A–A bond strength with increasing electronegativity difference ΔX between central atoms A and substituents B. An increase in ΔX tends to strengthen the A–A bond in the A_2B_4 and A_2B_6 classes. For example, the central bond in F_2B-BF_2 is much stronger than that in O_2N-NO_2. Larger ΔX increases the weighting and extent of hybridization of the central atom AOs in the orbitals responsible for net bonding in these systems. While the same rule holds for the 26-electron BAAB series, the reverse is true for the 18-electron examples. For instance, the central C–C bond in PCCP is stronger than that in NCCN for which ΔX is larger. The same principles apply in these cases but the rule reverses because of different properties of the MO that provides net bonding. The electronegativity rule is used to rationalize the nonexistence of certain compounds or to explain their preference for less symmetric structures.

We develop here a qualitative MO model[3] of the electronic structures of certain molecules and ions with the general formulas A_2B_{2n}. The model is based on extended Hückel calculations[4] for a number of different A_2B_2, A_2B_4, and A_2B_6 systems. The calculations and the qualitative model assume that MOs are formed from a basis set consisting of a single s

Table I. A_2B_4. 34 Valence Electron Series

	B_2F_4	$C_2O_4{}^{2-}$	N_2O_4	B_2Cl_4
$R(A-A)$, Å	1.75[a]	1.57[b]	1.78[c]	1.75[e]
$2r_A$, Å	1.60	1.54	1.48	1.60
Δr Å	0.15	0.03	0.30	0.15
$\angle BAB$, deg	120[a]	126[b]	134[c]	120[e]
$D(B_2A-AB_2)$, kcal/mol	88 ± 15		13[d]	83 ± 4
ΔX	2.0	0.9	0.4	1.1

[a] References 18 and 22. [b] Reference 10. [c] References 5 and 6.
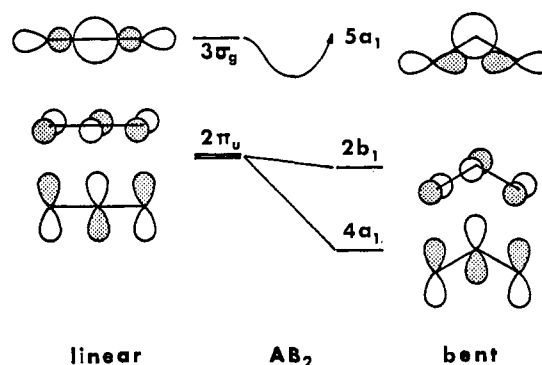[d] References 6 and 14. [e] References 24-26.

Figure 1. The relationships between some important AB_2 MOs in linear and bent geometry. The $4a_1$ orbital is less A–B antibonding than its $2\pi_u$ partner in linear geometry. The energy of $5a_1$ is strongly affected by mixing (not shown) with $4a_1$.

and three p AOs on each component atom. The A_2B_2 molecules and ions with 18 and 26 valence electrons, the A_2B_4 species with 34 and 38 electrons, and the 50-electron A_2B_6 series all have structures in which single bonds link AB_n monomers in symmetric dimers B_nA-AB_n. We show how trends in the A–A bond strength can be understood within the MO framework as a function of the electronegativity difference ΔX between central atoms A and substituent or terminal atoms B. We also use these trends to account for the nonexistence of some A_2B_{2n} compounds or to rationalize their preference for less symmetric structures. Electronegativity differences can also be invoked to explain what may be conformational differences between the isoelectronic molecules B_2F_4 and N_2O_4.

A_2B_4. Table I contains the A–A bond distances in some, A_2B_4 molecules and ions with 34 valence electrons. Two trends in this data are worthy of note. First, the A–A bond distance is longer for N_2O_4 than for $C_2O_4{}^{2-}$. One might expect the N–N distance to be shorter as a larger nuclear charge contracts the 2s and 2p valence AOs of the central atoms. The value $2r_A$, twice the covalent single bond radius of A, is smaller for N_2O_4 than for $C_2O_4{}^{2-}$. We use the quantity $\Delta r = R(A-A) - 2r_A$ to measure the deviation from the atomic radius additivity rule. One could hope that the radius additivity concept might apply through the series B_2F_4, $C_2O_4{}^{2-}$, and N_2O_4 since these species have the same set of MOs occupied by the same number of valence electrons. Compare the N–N single bond in N_2O_4 (1.78 Å)[5,6] with N–N single bonds in N_2F_4 (1.492 Å)[7,8] and N_2H_4 (1.449 Å). The B–B bond distance in B_2F_4 is probably more nearly a "normal" B–B distance than is twice the value quoted as the boron radius in most tables of covalent single-bond radii. Clearly, the C–C bond in $C_2O_4{}^{2-}$ (1.57 Å)[10] is rather long compared with single bonds in ethane (1.536 Å) and diamond (1.545 Å).[11] In summary, the central bond in $C_2O_4{}^{2-}$ is a little longer than expected and that in N_2O_4 is much longer. A second point of interest is the large difference in A–A bond strength between B_2F_4 and N_2O_4. We can correlate these trends in bond length and bond strength with the electronegativity difference ΔX between the central atoms A and the substituents B.

There is a third important anomaly in the A_2B_4 series. N_2O_4 is planar D_{2h} with a barrier to rotation about the N–N bond that is large (2–3 kcal/mol)[12,13] considering the long and weak (13 kcal/mol)[6,14] N–N bond. The Raman spectra of gaseous and solid B_2F_4 are consistent with a planar molecular structure in these states.[15] Previous infrared[16,17] and electron diffraction[18] studies were interpreted as indicating nonplanar, staggered D_{2d} geometry in the gas phase.[103] Ab initio SCF MO calculations favor the staggered conformation for B_2F_4.[19-21] All studies agree that the barrier to internal rotation about the B–B bond is small (0.5–1.8 kcal/mol). X-ray diffraction experiments show that B_2F_4 is planar in the solid.[22] B_2Cl_4[23-28] and B_2Br_4[29] are both staggered in the gas phase. In the crystalline state $C_2O_4{}^{2-}$ is usually planar but in some cases the two CO_2 groups may be twisted out of coplanarity by as much as 26°.[30] Vibrational spectra suggest that $C_2O_4{}^{2-}$ may be staggered in aqueous solutions.[31,32] Thus, molecules and ions

of the 34-electron A_2B_4 series may violate a Walsh-type rule that isoelectronic species should have the same molecular shape.[33] We show that the conformational trend in this series is also a function of the electronegativity difference between central atoms and substituents.

The 34 valence electrons of the A_2B_4 series occupy 17 molecular orbitals. The highest occupied MO is the σ-bonding MO $4a_g$. Among the 16 MOs of lower energy there are equal numbers of A–A bonding and A–A antibonding MOs. Thus, there is no net A–A bonding for A_2B_4 molecules with 32 valence electrons and, indeed, none are known with a direct A–A bond. Instead, the 32-electron molecules Be_2F_4[34] and Be_2Cl_4[35] apparently have planar D_{2h} structures that involve bridging atoms. If two 16-electron AB_2 monomers were brought together in coplanar fashion in an attempt to form an A–A link, not only would the A–A interactions be repulsive but the net out-of-phase interactions between B substituents on opposed monomers would be minimized if the monomers were rotated to the staggered D_{2d} conformation.

In the 34-electron planar D_{2h} system, the highest occupied MO, $4a_g$, is responsible for the symmetric A–A bonding of two AB_2 monomers. The $4a_g$ MO can be formed by the in-phase combination of two $4a_1$ MOs from a pair of bent (C_{2v}) AB_2 monomers. To develop an appreciation for the AO composition of the $4a_1$ MO and its position in energy relative to some vacant higher energy MOs, it will be necessary to see how the MOs of bent AB_2 relate to those of linear geometry. Figure 1 shows that $4a_1$ (C_{2v}) is related to the $2\pi_u$ MOs of linear ($D_{\infty h}$) AB_2. In a 16-electron AB_2 molecule such as CO_2 the $2\pi_u$ orbitals are empty and lower occupied MOs maintain linear geometry. The 17th electron that is present in BF_2, $CO_2{}^-$, and NO_2 goes into the $2\pi_u$ ($D_{\infty h}$)–$4a_1$ (C_{2v}) MO system. Bending removes the degeneracy of the completely antibonding $2\pi_u$ MOs. The in-phase π-type B—B overlap in $2b_1$ (C_{2v}) tends to lower slightly the energy of this orbital relative to $2\pi_u$ ($D_{\infty h}$). A much larger energy lowering occurs for $4a_1$ (C_{2v}) in which adjacent lobes on parallel p AOs that were A–B antibonding in $2\pi_u$ ($D_{\infty h}$) become A–B bonding in bent geometry. It is the $4a_1$ Mo that gives AB_2 molecules with 17-20 valence electrons their bent shape. In BF_2, $CO_2{}^-$, and NO_2, $4a_1$ is only singly occupied and the bond angles are rather wide, about 135° for NO_2[36] and $CO_2{}^-$.[37] The angle in BF_2 is apparently closer to 120°.[38] In AB_2 molecules with 18 electrons such as $NO_2{}^-$[39] and O_3,[40] $4a_1$ is doubly occupied and the bond angles are near 116°. In the coplanar dimerization of two 17-electron AB_2 monomers the singly occupied $4a_1$ MOs combine in-phase to form the doubly occupied $4a_g$ MO of A_2B_4 for net bonding and a stable dimer.

Considerations of electronegativity differences and orbital mixing produce modifications of $4a_1$ (AB_2) and $4a_g$ (A_2B_4).
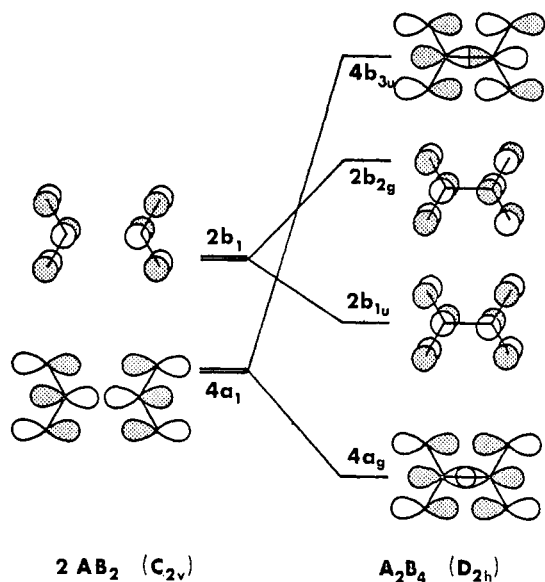
2 AB₂ **(C₂ᵥ)**　　　　　　**A₂B₄** **(D₂ₕ)**

Figure 2. MOs of two AB_2 monomers come together to form bonding and antibonding MOs of the dimer.
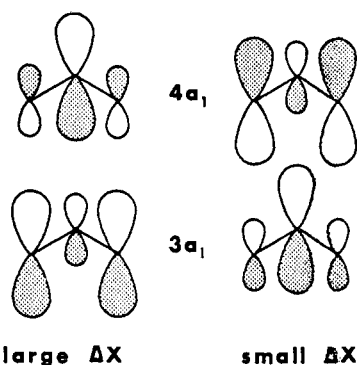

large ΔX　　　**small ΔX**

Figure 3. The effect on relative AO contributions of the electronegativity difference ΔX between central atom A and terminals B.

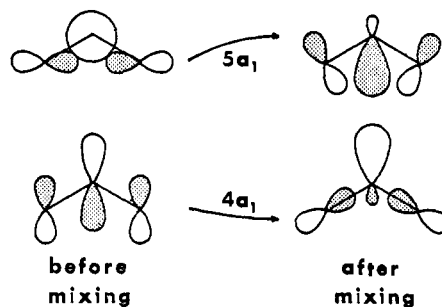**before**　　　　　**after**
mixing　　　　　**mixing**

Figure 4. The mixing of $4a_1$ and $5a_1$ gives added stability to $4a_1$ and produces a hybrid-type AO on the central atom capable of forming strong A-A bonds.
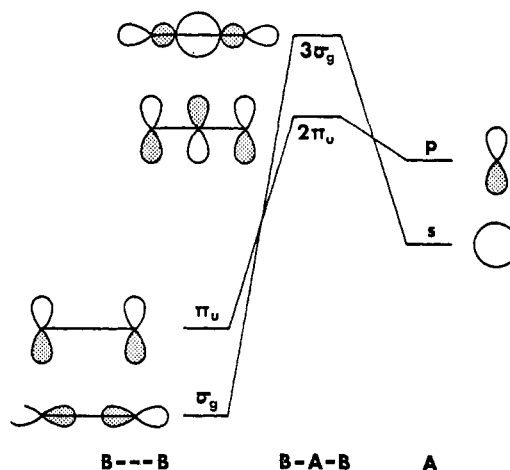

B---B　　**B-A-B**　　**A**

Figure 5. The higher the energy of the AOs of A, the weaker the interaction with the orbitals of B---B, narrowing the energy gap between $2\pi_u$ and $3\sigma_g(AB_2)$.
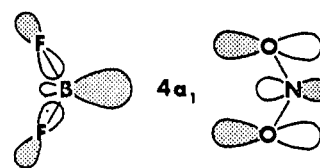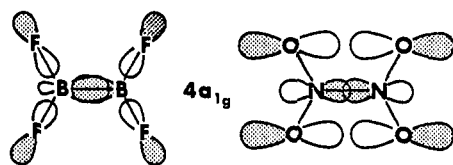

Figure 6. AO composition extremes in $4a_1$ (AB_2). BF_2 $(\Delta X$ large) and NO_2 $(\Delta X$ small).

In bent AB_2 the $3a_1$ and $4a_1$ MOs are composed primarily of parallel p AOs in the molecular plane. These are shown in Figure 3. Both $3a_1$ and $4a_1$ are related to components of the two π_u MOs of the linear AB_2 system. Suppose the central atom A is much less electronegative than the two terminals B, as in BF_2. Here we use electronegativity as a rough measure of the energies of the AOs. The contributions of the terminal p AOs in $3a_1$ would be large because these AOs have low energy and the contribution of the p orbital on the central atom would be small. The relative contributions of AOs in $4a_1$ would be just the opposite; this higher energy MO would be primarily the high energy p AO of the central atom with small coefficients for the p's on the terminals. As the electronegativity difference between the central atom and the terminals decreases, the situation reverses. Take O_3 for example. The central atom coefficient in $3a_1$ would be larger than those for the terminals, just as the lowest energy wave function for the particle in the one-dimensional box is higher in the center than at the ends. Again, the relative contributions of central atom and terminal atom p AOs are just the opposite in $4a_1$.

Lying above $4a_1$ in the MO systems of bent AB_2 is another orbital of a_1 symmetry. This MO, $5a_1$, is related to the $3\sigma_g$ MO of linear AB_2, as shown in Figure 1. Since $4a_1$ and $5a_1$ are close in energy and the highest energy MOs of a_1 symmetry they should mix as shown in Figure 4. The extent of this mixing will be greater the smaller the energy gap between $2\pi_u$ and $3\sigma_g$ $(D_{\infty h})$, the unmixable MOs of linear geometry from which $4a_1$ and $5a_1$ originate. Now the energy gap between $2\pi_u$ and $3\sigma_g$ is governed by the electronegativity difference between A and

B. Figure 5 shows how $2\pi_u$ and $3\sigma_g$ are formed by out-of-phase interactions between the s and p AOs of A and the symmetry-adapted orbitals of B---B, two substituent atoms separated by their distance in B-A-B. These B---b orbitals have energies that are slightly lower than those of pure p AOs on isolated substituent atoms. Consider BF_2 and NO_2 as extreme examples and assume linear geometry. The energies of the boron AOs are well above those of the fluorines since ΔX is large. Therefore, the antibonding perturbation interactions between π_u (B---B) and p(A) and between σ_g and s produce $2\pi_u$ and $3\sigma_g$ (AB_2), respectively, for BF_2 that are relatively close together in energy. For the NO_2 case (small ΔX) the B---B orbitals of oxygen fall between the s and p AOs of nitrogen and the resulting perturbation interactions are large, producing a larger energy gap between $2\pi_u$ and $3\sigma_g$. Therefore, the greater the difference in electronegativity between A and B, the greater the extent of mixing between $4a_1$ and $5a_1$.

The pictures of $4a_1$ for BF_2 and NO_2 in Figure 6 are exaggerated to emphasize AO composition differences due to electronegativity differences. In BF_2 the central atom p AO coefficient of $4a_1$ is large and the mixing with $5a_1$ is extensive, yielding a large sp-type hybrid orbital on boron pointing away from the vertex of the FBF angle. The small p AOs on the

Figure 7. AO composition extremes in $4a_g$ (A_2B_4).

Table II. A_2B_4. 38 Valence Electron Series

|	N_2F_4	P_2F_4	$S_2O_4{}^{2-}$
R(A–A), Å	1.49[a]	2.281[c]	2.389[d]
$2r_A$, Å	1.48	2.20	2.08
Δr, Å	0.01	0.08	0.31
D(B_2A–AB_2), kcal/mol	20.4[b]	57 ± 10[b]	21[e]
ΔX	0.9	1.8	0.8

[a] References 7 and 8. [b] Reference 46. [c] Reference 45. [d] Reference 43. [e] Reference 44.

fluorines point toward the rear nub of the boron hybrid. The extra stabilization of $4a_1$ due to mixing with $5a_1$ may account for the smaller angle in BF_2 compared to NO_2. For NO_2 the mixing between $4a_1$ and $5a_1$ is small (neglected all together in Figure 6), leaving $4a_1$ with a small p AO on the central N and large parallel p AOs on the terminal O's. Figure 7 combines the $4a_1$ MOs of AB_2 to form the bonding $4a_g$ of A_2B_4. The large hybrid orbitals pointing towards each other from the two borons form a strong B–B bond in B_2F_4. The small p AOs on the fluorines cannot interact strongly with those on the other end of the B–B bond. Net end–end antibonding interactions from the lower occupied MOs may dominate to give B_2F_4 the staggered conformation. In N_2O_4 the small nitrogen p AOs on the N–N axis overlap to form a weak dimer. On the other hand, large p AOs on the oxygens of opposite monomers overlap in phase to overcome the antibonding interactions of the lower orbitals and to stabilize a planar conformation for N_2O_4.

The rule of weaker central A–A bonds with decreasing electronegativity difference between A and B predicts that the B–B bond in B_2Cl_4 should be longer and weaker than that in B_2F_4. The experimental bond distances[24–26] and dissociation energies suggest that this might be true, although the large uncertainties in those values make the comparison questionable. However, the large size of the terminal atom AOs could also lengthen and weaken the B–B bond in B_2Cl_4 by increasing the out-of-phase interactions in the lower occupied valence MOs. In the series B_2F_4, $C_2O_4{}^{2-}$, and N_2O_4, all central atoms are from the same row of the periodic table and all terminals are also from the same row. For the comparison of B_2F_4 and B_2Cl_4 the terminals are from different rows. The higher principal quantum number of the valence AOs on chlorine gives those orbitals a larger effective radius, and therefore, the net antibonding or repulsive interactions from the 16 lower occupied MOs would be larger, lengthening and weakening the B–B bond of B_2Cl_4 compared to that of B_2F_4. These larger antibonding interactions are apparently responsible for the increase in the barrier to internal rotation from B_2F_4 (0.5 kcal/mol)[20] to B_2Cl_4 (1.5–2.5)[20,25–27] to B_2Br_4 (2.11–3.75).[29]

The electronegativity rule can also be used to rationalize the nonexistence of the thiooxalate anion, $C_2S_4{}^{2-}$. For this ion ΔX is smaller than that for N_2O_4 and one would predict an even weaker dimer bond. The larger sulfur atoms could also weaken the bond.

Note that we are not comparing the strengths of A–A bonds between elements from different rows of the periodic table. Such differences are not yet understood. For example, we do not claim that Al_2F_4 should be more strongly bound than B_2F_4,
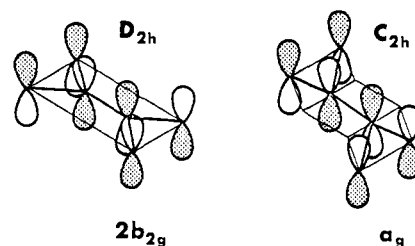
Figure 8. Folding causes parallel p AOs that are A–B antibonding in $2b_{2g}$ (D_{2h}) to become less so in a_g (C_{2h}), lowering the energy of the nonplanar structure. A similar effect occurs for $2b_{1u}$ (D_{2h}).
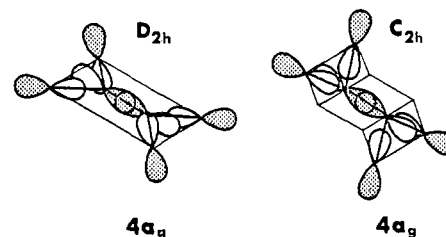
Figure 9. The AO composition of the $4a_g$ MO, responsible for A–A bonding in B_2F_4, is not greatly changed by folding to nonplanar geometry as in N_2F_4.

even though ΔX is larger in the Al_2F_4 case. Al_2F_4 is unknown. In fact, there are no known 34-electron A_2B_4 examples in which A is a second-row element.

The orbital $4a_g$ is formed by the in-phase combination of two $4a_1$ MOs from the AB_2 monomers. The corresponding out-of-phase combination $4b_{3u}$ is much higher in energy. Between $4a_g$ and $4b_{3u}$ lie $2b_{1u}$ and $2b_{2g}$, which are, respectively, the bonding and antibonding combinations of the $2b_1$ MOs of the AB_2 monomers. Refer once more to Figure 2. The $2b_{1u}$ MO makes the π bond in 36-electron molecules such as C_2F_4. In 38-electron molecules the antibonding $2b_{2g}$ MO is occupied, canceling the π bond and yielding another A–A single-bonded series that includes N_2F_4 and $S_2O_4{}^{2-}$. If 40 electrons were to occupy this MO system, the antibonding $4b_{3u}$ orbital would be filled, canceling the σ A–A link of $4a_g$. The 40-electron molecule S_2F_4 is known[41] but it has the unsymmetrical structure F_3S–SF rather than the symmetrical B_2AAB_2 pattern that is ruled out by MO considerations.

The A_2B_4 class contains two series of singly bonded dimers. Molecules in the 38-electron series have nonplanar trans C_{2h} conformations with possible rotational isomers of gauche C_2 symmetry. An explanation of the rotational conformations is the subject of another story[42] but it is easy to see from Figure 8 why the B_2A–AB_2 system prefers to be nonplanar with 38 electrons. Out-of-plane folding changes the $2b_{1u}$ and $2b_{2g}$ MOs from A–B antibonding orbitals of planar geometry to A–B bonding orbitals of pyramidal geometry about A. Orbital overlaps change in exactly the same way as for the conversion of $2\pi_u$ (AB_2, $D_{\infty h}$) into $4a_1$ (AB_2, C_{2v}) shown in Figure 1. Folding the A_2B_4 structure to trans shape changes $4a_g$ (D_{2h}) into $4a_g$ (C_{2h}). Thus, the $4a_g$ MOs that are responsible for A–A bonding in both the 34 (D_{2h}) and 38 (C_{2h}) electron series are directly related through AO composition, as shown in Figure 9, and the same electronegativity rule applies. Table II contains data for some 38-electron A_2B_4 molecules. As expected the A–A bond in $S_2O_4{}^{2-}$[43,44] is longer and weaker than that in P_2F_4.[45,46] There is some uncertainty about the electronegativity rule in the diphosphines. Estimates of P–P bond energies seem to increase through the series P_2F_4 (57 ± 10 kcal/mol), P_2Cl_4 (62), P_2I_4 (71–80),[46] but the uncertainties in these estimates are quite large. The P–P bond distance in P_2F_4 (2.28 Å)[45] is longer than that in P_2I_4 (2.21 Å).[47] On the

Table III. A_2B_6. 50 Valence Electron Series

	Si_2F_6	$P_2O_6{}^{4-}$	$S_2O_6{}^{2-}$	Si_2Cl_6	$P_2S_6{}^{4-}$	$P_2Se_6{}^{4-}$
$R(A-A)$, Å	2.32[a]	2.17[b]	2.15[c]	2.32[d]	2.20[e]	2.24[e]
$2r_A$, Å	2.34	2.20	2.08	2.34	2.20	2.20
Δr, Å	−0.02	−0.03	+0.07	−0.02	0	0.04
ΔX	2.1	1.2	0.8	1.2	0.4	0.4

[a] Reference 75. [b] Reference 67. [c] Reference 76. [d] J. Haase, Z. *Naturforsch. A*, **28**, 542 (1973). [e] Reference 68.
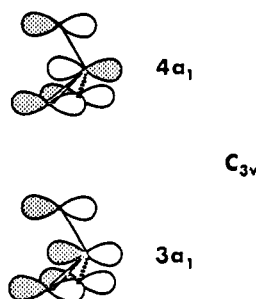

Figure 10. The $3a_1$ and $4a_1$ MOs of pyramidal AB_3 are formed from parallel p AOs, just like $3a_1$ and $4a_1$ in AB_2.

other hand, the calculated P-P stretching force constant for P_2Cl_4 is greater than that for P_2I_4.[48] The compounds X_2O_4 (X = halogen) are known. A study of the MOs for AB_2 molecules concludes that those orbitals with considerable end-atom character (because of nodes passing through the central atom) are much more stable if the more electronegative element occupies a terminal position.[49] Thus, the expected arrangement of O_2F is FOO, which has been observed experimentally,[50] rather than OFO, which is unknown. Even assuming an OFO monomer, the ΔX rule would not predict a stable dimer O_2F-FO_2 for which the central atoms are highly electronegative compared to the terminals. Instead, F_2O_4 has the peroxide-type structure FOOOOF.[51] The electronegativities of Cl and O are close ($\Delta X = 0.3$) and one would not expect a strong Cl-Cl bond in Cl_2O_4. Instead, this compound has the unsymmetrical structure $O_3Cl-O-Cl$.[52] Symmetrical Br_2O_4 is more likely since ΔX is larger (0.5) and indeed vibrational spectra favor the structure $O_2Br-BrO_2$.[53] The Mossbauer spectrum of I_2O_4 in frozen H_2SO_4 solution suggests O_2IO^--IO^{+}[54], which is related to the structure of the polymeric solid.[55] Our electronegativity rule predicts a symmetrical structure because ΔX is larger (0.8) than for Br_2O_4. Finally, N_2O_4 and N_2F_4 offer one comparison between the 34- and 38-electron series. The larger electronegativity difference in N_2F_4 makes its N-N bond shorter and stronger[56] than that in N_2O_4.

A_2B_6. Table III lists some known ethanelike A_2B_6 molecules and ions containing 50 valence electrons. These electrons occupy 25 MOs, the highest of which is the A-A σ bonding $4a_{1g}$ MO. Below $4a_{1g}$ lie 24 MOs among which are equal numbers of A-A bonding and A-A antibonding orbitals. The net effect of these 24 underlying MOs is therefore repulsive, giving 50-electron molecules their staggered D_{3d} conformation. Although there are many 48-electron A_2B_6 molecules, none has a direct A-A bond between the two AB_3 monomers. Instead, the 48-electron molecules have diborane-like structures with a pair of bridging atoms. Examples are Al_2I_6,[57] Ga_2Cl_6,[58] and $Ge_2S_6{}^{4-}$.[59]

The $4a_{1g}$ MO of A_2B_6 forms the bond between two AB_3 monomers. This MO is the in-phase combination of singly occupied $4a_1$ MOs of the two AB_3 monomers. The $4a_1$ MO gives 25- and 26-electron AB_3 molecules their pyramidal (C_{3v}) shape as shown in Figure 10. The change from planar to pyramidal shape moves parallel p AOs from A-B antibonding

positions into A-B bonding positions, just like that for $4a_1$ (AB_2, C_{2v}). Compare Figures 1 and 10. Furthermore, the same relationship holds between the $3a_1$ and $4a_1$ MOs of AB_3 that we found for the $3a_1$ and $4a_1$ MOs of AB_2. Both sets consist of p AOs that lie parallel to the rotational axis of the monomer. Therefore, there is a direct relationship between $4a_{1g}$ (A_2B_6) and $4a_g$ (A_2B_4) and the electronegativity rule that we found for 34- and 38-electron A_2B_4 molecules holds for the 50-electron A_2B_6 series as well.

The only A-A bond energy comparison for the 50-electron A_2B_6 series is between C_2F_6 (96.5 kcal/mol)[60] and C_2Cl_6 (72.4).[61] However, the substituents have valence AOs of different principal quantum number and the larger substitutent AOs could also act to weaken the C-C bond. Larger substituent orbitals are presumably responsible for the increasing barrier to internal rotation from C_2F_6 (3.91 kcal/mol)[62] to C_2Cl_6 (10.8-17.5)[63] to C_2Br_6 (13-50?).[64] Most comparisons of A-A bond distances are for systems in which variations might be due to both the electronegativity rule and substituent orbital size. The two series $Ga_2Cl_6{}^{2-}$ (2.390 Å),[65] $Ga_2Br_6{}^{2-}$ (2.419)[66] and $P_2O_6{}^{4-}$ (2.17),[67] $P_2S_6{}^{4-}$ (2.20), $P_2Se_6{}^{4-}$ (2.24)[68] show clear lengthening of the central A-A bond with increasing substituent orbital size and decreasing ΔX. The difference of 0.02 Å between observed C-C bond distances in C_2F_6 (1.545 Å)[69] and C_2Cl_6 (1.564)[70] is surprisingly small considering the 24 kcal/mol difference in dissociation energies $D(X_3C-CX_3)$. The reported C-C bond distance in C_2Br_6 (1.526 Å)[71] is shorter than that in either C_2F_6 or C_2Cl_6. However, these central bond distances are difficult to measure accurately by x-ray or electron diffraction techniques because the two carbons are virtually surrounded and, therefore, obscured by six strongly scattering halogen atoms.

Another measure for the comparison of A-A bond strengths is calculated A-A stretching force constants. A pattern of decreasing Si-Si stretching force constants has been observed in the Si_2X_6 series: Si_2F_6 (2.4 mdyn/Å), Si_2Cl_6 (2.4), Si_2Br_6 (2.1), Si_2I_6 (1.9).[72] The In-In stretching constants in $In_2X_6{}^{2-}$ seem to follow a similar trend: $In_2Cl_6{}^{2-}$ (0.64 ± 0.08 mdyn/Å), $In_2Br_6{}^{2-}$ (0.69 ± 0.06), $In_2I_6{}^{2-}$ (0.24 ± 0.01).[73] One might hope to find the same pattern for the C-C stretches in the perhaloethanes C_2X_6. The vibrational spectral data are available but apparently force constants for this series have never been calculated without the assumption of equal C-C stretching force constants throughout.[74]

In the series Si_2F_6,[75] $P_2O_6{}^{4-}$, $S_2O_6{}^{2-}$,[76] and Cl_2O_6 all central atoms A come from the same row of the periodic table and all substituents B come from the same row. Therefore, it should be possible to isolate the effect of electronegativity differences on A-A bond strengths or distances. Table III compares the observed bond distances $R(A-A)$ with twice the covalent radii $2r_A$. The difference $\Delta r = R(A-A) - 2r_A$ is a measure of the deviation of $R(A-A)$ from the radius additivity rule. For Si_2F_6 and $P_2O_6{}^{4-}$, Δr is negligible, the negative value perhaps indicating that the A-A distance is even a little shorter than predicted by the radius additivity rule. The small value and negative sign of Δr for $P_2O_6{}^{4-}$ also eases concern that the large charge in this ion might produce an expansion of the ion and a lengthening of the P-P bond. The value of $\Delta r = +0.07$ Å for $S_2O_6{}^{2-}$ signals a lengthening of the S-S bond. The

Table IV. S_2X_2. 26 Valence Electron Series

	S_2F_2	S_2Cl_2	S_2Br_2	S_4^{2-}
$R(S-S)$, Å	1.89[b]	1.93[c]	1.98[d]	2.07[e]
Δr, Å[a]	−0.19	−0.15	−0.10	−0.01
ΔX	1.4	0.6	0.4	0

[a] $2r_s = 2.08$ Å. [b] Reference 83. [c] Reference 84. [d] Reference 85. [e] Reference 93.

compound Cl_2O_6 has long been known.[77] ΔX is very small. Recent spectroscopic measurements of the liquid indicate that the ClO_3 dimer is not symmetric or ethanelike but rather it has the unsymmetrical structure $O_3Cl-O-ClO_2$.[78]

A_2B_2. Both the 18- and the 26-electron series of the BAAB class have A–A single bonds. Members of the 18-electron series are C_2N_2, C_2P_2, B_2O_2, and B_2S_2. C_2N_2 has a linear symmetric structure $N\equiv C-C\equiv N$ and bond distances are known accurately from x-ray diffraction measurements.[79] The infrared spectrum of B_2O_2 is consistent with a linear symmetric molecule $OBBO$[80] and this is the structure we assume, although thermodynamic data have recently been used to argue in favor of a bent unsymmetrical molecule.[81] The 26-electron series includes O_2F_2,[82] S_2F_2,[83] S_2Cl_2,[84] S_2Br_2,[85] Se_2Cl_2,[86] and Se_2Br_2.[86] These molecules are known to have chainlike, nonplanar, gauche C_2 shapes like hydrogen peroxide. The molecule S_2I_2 is stable only at low temperatures. Its structure is unknown.[87] The shapes of A_2B_2 molecules and ions have been discussed in detail elsewhere.[88]

The members of the 26-electron series seem to follow the electronegativity rule for A–A bond strengths that we have developed for single bonded A_2B_4 and A_2B_6 systems. The data in Table IV show that the S–S bond grows longer through the series S_2F_2, S_2Cl_2, S_2Br_2 as ΔX decreases. For O_2F_2 the dissociation energy $D(FO-OF)$ is estimated to be 62.1 kcal/mol.[89] The Cl_2O_2 dimer, however, is very weakly bound and it possibly has the unsymmetrical structure $ClO-ClO$.[90] The 26-electron homonuclear ions S_4^{2-} and I_4^{2+} are weakly bound as the electronegativity rule would predict. The dissociation energy of I_4^{2+} into $2I_2^+$ is estimated to be 10 kcal/mol.[91] In liquid solutions S_4^{2-} is in equilibrium with the radical ions $2S_2^-$.[92] The x-ray crystal structure of BaS_4 has been determined[93] and the central S–S bond in the S_4^{2-} ion is long (2.07 Å) compared to that in S_2Cl_2 (1.93 Å), a molecule containing terminal atoms of greater electronegativity but with valence AOs of the same principal quantum number as the sulfur terminals in the homonuclear ion S_4^{2-}. In contrast, the 18-electron series does not appear to follow the electronegativity rule. It turns out that exactly the same principles apply but the result is a reversal of the effect for the linear 18-electron series. The electronegativities of C and N are fairly close, yet the central bond in $N\equiv C-C\equiv N$ has a dissociation energy of 128 kcal/mol,[94] very strong and short (1.38 Å) compared to the C–C bond in C_2F_6 (96.5 kcal/mol; 1.545 Å). Apparently the central bond in $OB-BO$ is weaker than that in $NC-CN$ despite the larger electronegativity difference ΔX between B and O than between C and N. Estimates of $D(OB-BO)$ range from 100 to 120 kcal/mol.[80,95] The B–B distance in B_2O_2 is unknown. From the heats of atomization of CP and C_2P_2[96] one can calculate $D(PC-CP) = 149 \pm 8$ kcal/mol. In this case, ΔX is smaller than for C_2N_2 and the carbon–carbon bond is stronger.

Figure 11 shows some of the higher energy valence MOs for linear BAAB. Molecular shapes and qualitative MOs for the BAAB class have been discussed in detail elsewhere.[88] In the 18-electron BAAB series the highest occupied MO is the $3\sigma_g$ orbital formed by the in-phase overlap of the collinear p AOs on the four atoms BAAB. Below $3\sigma_g$, 16 electrons occupy 8 MOs of which half are A–A bonding and half are A–A anti-
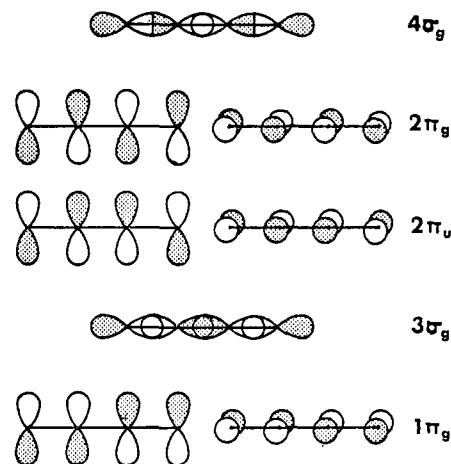

Figure 11. Some of the valence MOs of linear A_2B_2. The $3\sigma_u$ MO that lies between $2\pi_g$ and $4\sigma_g$ has been omitted here because it plays no part in our discussion.
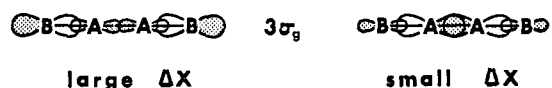

Figure 12. Relative AO compositions in $3\sigma_g$ for extremes in ΔX. Smaller ΔX forms the stronger A–A bond.

bonding. Thus, it is $3\sigma_g$ that provides the A–A single bond which links the two AB monomers in the linear A_2B_2 dimer. As just stated our model would not account for 16-electron A_2B_2 species with a direct A–A bond. In fact, C_4 (16 electrons) has been detected in the vapor over graphite at high temperatures. The abundance of C_4 is less than that of either C_3 or C_5.[97] Now $3\sigma_g$ and $1\pi_g$ are close in energy and their order is poorly determined by qualitative considerations. They might be reversed in the case of C_4. If $3\sigma_g$ were below $1\pi_g$ then two C_2 monomers would be joined by the bonding $3\sigma_g$ MO and C_4 would be an open shell or triplet state because $1\pi_g$ would be only half filled, a configuration supported by the calculations of Pitzer and Clementi.[98]

For large ΔX the p AOs from the terminal B atoms would make the larger contribution to $3\sigma_g$ because the B atom p's have lower energy than those from the central atoms A. For small ΔX the central A–A p contributions are large, again by analogy with the lowest energy wave function for the particle in the one-dimensional box. Figure 12 illustrates these two extremes. The larger the p coefficients on A, the stronger the A–A bond. Thus, for larger ΔX we predict weaker A–A bonds for the linear 18-electron series.

Moving from the 18-electron A_2B_2 series to the 26-electron series, 8 electrons are added to two sets of doubly degenerate MOs, $2\pi_u$ and $2\pi_g$. The A–A bonding character of the $2\pi_u$ orbitals is canceled by the antibonding nature of $2\pi_g$ and therefore the 26-electron series should have A–A single bonds, which they do. If that single bond were due to the same $3\sigma_g$ MO responsible for bonding in the 18-electron series, then one would expect weaker A–A bonds for larger ΔX, a trend opposite to that observed for the 26-electron series. The resolution of this dilemma is based on the fact that the 26-electron molecules are not linear. Although the 26-electron species are actually nonplanar or gauche C_2, we assume planar, trans C_{2h} geometry for representational convenience. If $3\sigma_g$ were bent trans, one would expect its energy to rise because collinear p AO overlaps between atoms A and B would be reduced. Above $2\pi_g$ is $4\sigma_g$, the A–B antibonding combination of collinear p AOs related to $3\sigma_g$. On bending, the energy of $4\sigma_g$ ought to lower because A–B out-of-phase overlaps are relaxed. Both $3\sigma_g$ and $4\sigma_g$ produce MOs of a_g symmetry in trans geometry. Bending produces a reversal of order of the two a_g MOs derived
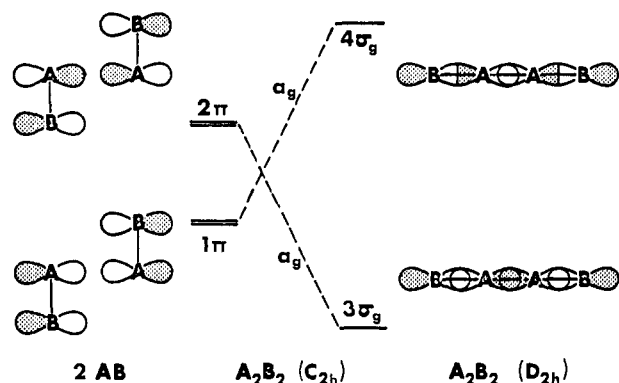
Figure 13. The intended correlations of π MOs of trans-oriented AB monomers with the σ MOs of the linear dimer A_2B_2.

from $3\sigma_g$ and $4\sigma_g$. That this must be so can be seen from Figure 13, in which these same MOs are formed through in-phase combinations of the appropriate MOs of two AB monomers to form directly the trans-bent dimer. Figure 13 shows that by the in-phase combination of two A–B bonding 1π MOs of trans associated AB monomers one can form an a_g dimer orbital that has the same phase relationships among component p AOs as those in $4\sigma_g$ of the linear structure. Similarly, the in-phase combination of two antibonding 2π MOs of AB monomers leads to the $3\sigma_g$ MO of the linear dimer. The dashed lines connecting 1π (AB) and $4\sigma_g$ (A_2B_2) and between 2π (AB) and $3\sigma_g$ (A_2B_2) represent intended correlations that are not allowed by the noncrossing rule. The actual picture is even more complicated because of the mixing of other MOs of a_g symmetry since there are six a_g MOs that can be made from our AO basis set. The a_g MO that maintains net A–A bonding in the nonlinear 26-electron series is that made by combining the two 2π (AB) MOs. It is, after all, related to $3\sigma_g$ (A_2B_2) by AO phases. But Figure 13 shows how the a_g MO related to $4\sigma_g$ (A_2B_2) slips underneath in nonlinear geometry.

Now consider how the 1π and 2π MOs of the AB monomer are influenced by ΔX. As for AB_2 (Figure 3) and AB_3 (Figure 10), we are concerned with a pair of monomer MOs formed from parallel p AOs. If ΔX is zero (homonuclear case) the two p AO coefficients must be equal in both 1π and the higher energy 2π. If ΔX is large then the p AO contribution of B in 1π will be larger than that of A because the AO energies of B are lower. Conversely, the p AO contribution from A will be larger in the higher energy combination 2π. Figure 14 protrays the extreme cases. Since the size of the A atom p contribution determines the strength of the A–A bond, then large ΔX systems will form strong A–A bonds, just as they did in the A_2B_4 and A_2B_6 classes. There is a difference, however. For $\Delta X = 0$, the A and B p AO coefficients in 2π must be equal; small ΔX does not diminish the A atom p contribution below that of the B atom, a consequence that can occur in the comparable MOs of AB_2 and AB_3. The requirement that the p contribution from A to 2π cannot be smaller than that from B, therefore, limits the weakening suffered by the BA–AB bond for small ΔX cases and accounts for the existence of homonuclear ions S_4^{2-} and I_4^{2+} which have no counterparts in the A_2B_4 and A_2B_6 classes.

Semiquantitative Comparisons. The conclusions of the qualitative arguments agree with the results of extended Hückel calculations. For example, as ΔX increases (as reflected in the calculations by differences in input parameters for atomic ionization potentials) there is an increase in the ratio of the s AO coefficient to the p coefficient for the central atom A in the $4a_1$ orbital of bent AB_2, indicating a greater extent of hybridization of the central atom AOs as represented in Figure 6. Larger ΔX also produces greater A–A bond orders and smaller end-end B---B bond orders in the $4a_g$ MO of
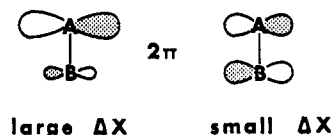

Figure 14. Relative AO compositions of the 2π MO of the AB monomer, assuming the electronegativity of B to be greater than or equal to that of A.

planar A_2B_4 as shown in Figure 7. The energy order of the MOs pictured in Figure 2 agrees with the order of MOs for B_2F_4, $C_2O_4^{2-}$, and N_2O_4 obtained by extended Hückel calculations. Calculations for A_2B_6 and A_2B_2 classes lend similar support to the qualitative arguments for those systems.

The calculated relative order of the $1\pi_g$ and $3\sigma_g$ MOs for linear BAAB molecules depends on the parameter values used in the calculations. Similar difficulties occur in the ordering of the $1\pi_g$ and $2\sigma_u$ orbitals of linear AB_2 and the $1\pi_u$ and $2\sigma_g$ orbitals of A_2. A reversal of the order of $1\pi_g$ and $3\sigma_g$ does not affect the qualitative conclusions about A–A bond strengths in the 18-electron BAAB series. In the other cases studied here the agreement between energy level orderings obtained by qualitative arguments and by semiquantitative calculations is excellent.

Other Models. Several papers by other investigators have an important relationship to this work. Brown and Harcourt have studied the strengths of A–A bonds in the 34-, 36-, and 38-valence electron A_2B_4 series.[99] They too note weaker A–A bonds as A and B approach each other in electronegativity, a trend that is in accord with A–A bond populations from their semiempirical MO calculations. They explain that the trend results from the delocalization of lone pairs of the B atoms into the A–A σ-antibonding MO. Harcourt has rationalized bond properties in A_2B_4 molecules in terms of expanded valence electron dot diagrams.[100] Moore[101] was the first to do extended Hückel calculations for B_2F_4 and N_2O_4 in planar and staggered conformations. His calculated bond populations reflect a strong B–B bond in B_2F_4, a slightly weaker bond in B_2Cl_4, and a considerably weaker bond in N_2O_4. Furthermore, bond populations between substituents on opposite monomers are weak in B_2F_4 but considerably larger in N_2O_4. Redmond and Wayland[102] performed extended Hückel calculations for NO_2 and N_2O_4 and recognized $4a_g$ as the MO responsible for the dimerization of NO_2. Bibart and Ewing[12] include pictures of the $4a_1$ MOs of two NO_2 monomers and the $4a_g$ MO of N_2O_4 which are very similar to those in Figures 6 and 7 of this paper. They use those diagrams to rationalize the planar conformation of N_2O_4. Howell and Van Wazer[21] have done both extended Hückel and ab initio SCF MO calculations to study conformational differences between B_2F_4 and N_2O_4. Although their qualitative interpretation is somewhat different from ours, the two explanations are in no way contradictory. A strengthening of central bonds by more electronegative substituents has been noted by Bartell,[45] who also pointed out that this rule may fail for diphosphines. Höfler, Sawodny, and Hengge[72] have described the declining Si–Si stretching force constants with decreasing electronegativity of substituent in perhalodisilanes. Beagley and co-workers pointed out the electronegative substituent effect of shortened S–S bonds in the series S_2X_2.[84] Our work provides a qualitative MO framework that helps rationalize these various observations and calculations.

References and Notes

(1) A preliminary version of this paper was presented at the 26th Southeastern Regional Meeting of the American Chemical Society, Norfolk, Va., Oct 23–25, 1974, Paper No. 169.
(2) To whom correspondence should be addressed.

(3) B. M. Gimarc, *Acc. Chem. Res.*, **7**, 384 (1974).
(4) R. Hoffmann, *J. Chem. Phys.*, **39**, 1397 (1963).
(5) B. W. McClelland, G. Gundersen, and K. Hedberg, *J. Chem. Phys.*, **56**, 4541 (1972).
(6) Q. Shen, *Diss. Abstr. Int. B*, **34**, 3735 (1974).
(7) M. J. Cardillo and S. H. Bauer, *Inorg. Chem.*, **8**, 2086 (1969).
(8) M. M. Gilbert, G. Gundersen, and K. Hedberg, *J. Chem. Phys.*, **56**, 1691 (1972).
(9) Y. Morino, T. Iijima, and Y. Murata, *Bull. Chem. Soc. Jpn.*, **33**, 46 (1960).
(10) B. F. Pederson, *Acta Chem. Scand.*, **18**, 1635 (1964); B. Beagley and R. W. H. Small, *Acta Crystallogr.*, **17**, 783 (1964); D. J. Hodgson and J. A. Ibers, *Acta Crystallogr., Sect B*, **25**, 469 (1969).
(11) L. E. Sutton, Ed., *Chem. Soc., Spec. Publ.*, **No. 11** (1958); **No. 18** (1965).
(12) C. H. Bibart and G. E. Ewing, *J. Chem. Phys.*, **61**, 1284 (1974).
(13) R. G. Snyder and I. C. Hisatsune, *J. Mol. Spectrosc.*, **1**, 139 (1957).
(14) I. C. Hisatsune, *J. Phys. Chem.*, **65**, 2249 (1961).
(15) J. R. Durig, J. W. Thompson, J. D. Witt, and J. D. Odom, *J. Chem. Phys.*, **58**, 5339 (1973).
(16) J. N. Gayles and J. Self, *J. Chem. Phys.*, **40**, 3530 (1964).
(17) L. A. Nimon, K. S. Seshadri, R. C. Taylor, and D. White, *J. Chem. Phys.*, **53**, 2416 (1970).
(18) J. V. Patton and K. Hedberg, *Bull. Am. Phys. Soc.*, **13**, 831 (1968).
(19) N. J. Fitzpatrick, *Inorg. Nucl. Chem. Lett.*, **9**, 965 (1973).
(20) M. F. Guest and I. H. Hillier, *J. Chem. Soc., Faraday Trans. 2*, **70**, 398 (1974).
(21) J. M. Howell and J. R. Van Wazer, *J. Am. Chem. Soc.*, **96**, 7902 (1974).
(22) L. Trefonas and W. N. Lipscomb, *J. Chem. Phys.*, **28**, 54 (1958).
(23) J. R. Durig, J. E. Saunders, and J. D. Odom, *J. Chem. Phys.*, **54**, 5285 (1971).
(24) M. Atoji, P. J. Wheatley, and W. N. Lipscomb, *J. Chem. Phys.*, **27**, 196 (1957).
(25) K. Hedberg and R. R. Ryan, *J. Chem. Phys.*, **41**, 2214 (1964).
(26) R. R. Ryan and K. Hedberg, *J. Chem. Phys.*, **50**, 4986 (1969).
(27) L. H. Jones and R. R. Ryan, *J. Chem. Phys.*, **57**, 1012 (1972).
(28) D. E. Mann and L. Fano, *J. Chem. Phys.*, **26**, 1665 (1957).
(29) J. D. Odom, J. E. Saunders, and J. R. Durig, *J. Chem. Phys.*, **56**, 1643 (1972).
(30) J. H. Robertson, *Acta Crystallogr.*, **18**, 410 (1965).
(31) M. J. Schmelz, T. Miyazawa, S.-I. Mizushima, T. J. Lane, and J. V. Quagliano, *Spectrochim. Acta*, **9**, 51 (1957).
(32) G. M. Begun and W. H. Fletcher, *Spectrochim. Acta*, **19**, 1343 (1963).
(33) P. J. Wheatley, *J. Chem. Soc.*, 4514 (1956).
(34) A. Snelson, B. N. Cyvin, and S. J. Cyvin, *Z. Anorg. Allg. Chem.*, **410**, 206 (1974).
(35) A. Büchler and W. J. Klemperer, *J. Chem. Phys.*, **29**, 121 (1958); G. A. Ozin, *Prog. Inorg. Chem.*, **14**, 173 (1971).
(36) K.-E. J. Hallin and A. J. Merer, *Can. J. Phys.*, **54**, 1157 (1976); C. F. Jackels and E. R. Davidson, *J. Chem. Phys.*, **65**, 2941 (1976).
(37) D. W. Ovenall and D. H. Whiffen, *Mol. Phys.*, **4**, 135 (1961); J. Pacansky, U. Wahlgren, and P. S. Bagus, *J. Chem. Phys.*, **62**, 2740 (1975).
(38) W. Nelson and W. Gordy, *J. Chem. Phys.*, **51**, 4710 (1969); C. Thomson and D. A. Brotchie, *Theor. Chim. Acta*, **32**, 101 (1973).
(39) E. Herbst, T. A. Patterson, and W. C. Lineberger, *J. Chem. Phys.*, **61**, 1300 (1974); G. V. Pfeiffer and L. C. Allen, *ibid.*, **61**, 190 (1969).
(40) R. H. Hughes, *J. Chem. Phys.*, **24**, 131 (1956).
(41) F. Seel, R. Budenz, and W. Gombler, *Chem. Ber.*, **103**, 1710 (1970); F. Seel and R. Budenz, *J. Fluorine Chem.*, **1**, 117 (1971).
(42) J. R. Durig, B. M. Gimarc, and J. D. Odom, *Vib. Spectra Struct.*, **2**, 1 (1973).
(43) J. D. Dunitz, *J. Am. Chem. Soc.*, **78**, 878 (1956); J. D. Dunitz, *Acta Crystallogr.*, **9**, 579 (1956).
(44) L. Burlamacchi, G. Casini, O. Fagioli, and E. Tiezzi, *Ric. Sci.*, **37**, 97 (1967).
(45) H. L. Hodges, L. S. Su, and L. S. Bartell, *Inorg. Chem.*, **14**, 599 (1975).
(46) C. R. S. Dean, A. Finch, P. J. Gardner, and D. W. Payling, *J. Chem. Soc., Faraday Trans. 1*, **70**, 1921 (1974).
(47) Y. C. Leung and J. Waser, *J. Phys. Chem.*, **60**, 539 (1956).
(48) G. Shanmugasundaram and G. Nagarajan, *Monatsh. Chem.*, **100**, 789 (1969).
(49) R. J. Buenker and S. D. Peyerimhoff, *Chem. Rev.*, **74**, 127 (1974).
(50) P. N. Noble and G. C. Pimentel, *J. Chem. Phys.*, **44**, 3641 (1966).
(51) A. V. Grosse, A. G. Streng, and A. D. Kirshenbaum, *J. Am. Chem. Soc.*, **83**, 1004 (1961); A. Arkell, *ibid.*, **87**, 4057 (1965); B. Plesnicar, D. Kocjan, S. Murovec, and A. Azman, *ibid.*, **98**, 3143 (1976).
(52) C. J. Schack and D. Pilipovich, *Inorg. Chem.*, **9**, 1387 (1970); K. O. Christe, C. J. Schack, and E. C. Curtis, *ibid.*, **10**, 1589 (1971).
(53) J.-L. Pascal and J. Potier, *J. Chem. Soc., Chem. Commun.*, 446 (1973).
(54) C. H. W. Jones, *J. Chem. Phys.*, **62**, 4343 (1975).
(55) W. E. Dasent and T. C. Waddington, *J. Chem. Soc.*, 3550 (1960).
(56) S. N. Foner and R. L. Hudson, *J. Chem. Phys.*, **58**, 581 (1973).
(57) K. J. Palmer and N. Elliot, *J. Am. Chem. Soc.*, **60**, 1852 (1938).
(58) S. C. Wallwork and I. J. Worrall, *J. Chem. Soc.*, 1816 (1965).
(59) B. Krebs, S. Pohl, and W. Schiwy, *Z. Anorg. Allg. Chem.*, **393**, 341 (1972).
(60) J. W. Coomber and E. Whittle, *Trans. Faraday Soc.*, **63**, 1394 (1967).
(61) J. A. Franklin and G. H. Huybrechts, *Int. J. Chem. Kinet.*, **1**, 3 (1969).
(62) D. F. Eggers, Jr., R. C. Lord, and C. W. Wickstrom, *J. Mol. Spectrosc.*, **59**, 63 (1976).
(63) D. A. Swick, I. L. Karle, and J. Karle, *J. Chem. Phys.*, **22**, 1242 (1954); Y. Morino, *ibid.*, **28**, 185 (1958); J. Karle, *ibid.*, **45**, 4149 (1966); G. Allen, P. N. Brier, and G. Lane, *Trans. Faraday Soc.*, **63**, 824 (1967).
(64) G. Heublein, R. Kühmstedt, P. Kadura, and H. Dawczynski, *Tetrahedron*, **26**, 81 (1970).
(65) K. L. Brown and D. Hall, *J. Chem. Soc., Dalton Trans.*, 1843 (1973).
(66) H. J. Cumming, D. Hall, and C. E. Wright, *Cryst. Struct. Commun.*, **3**, 103 (1974).
(67) A. Wilson and H. McGeachin, *Acta Crystallogr.*, **17**, 1352 (1964).
(68) W. Klinger, G. Eulenberger, and H. Hahn, *Z. Anorg. Allg. Chem.*, **401**, 97 (1973).
(69) K. L. Gallaher, A. Yokozeki, and S. H. Bauer, *J. Phys. Chem.*, **78**, 2389 (1974).
(70) A. Almenningen, B. Andersen, and M. Traetteberg, *Acta Chem. Scand.*, **18**, 603 (1964).
(71) G. Mandel and J. Donohue, *Acta Crystallogr., Sect. B*, **28**, 1313 (1972).
(72) F. Höfler, W. Sawodny, and E. Hengge, *Spectrochim. Acta, Part A*, **26**, 819 (1970); E. Hengge, *Monatsh. Chem.*, **102**, 734 (1971); F. Höfler, S. Waldhör, and E. Hengge, *Spectrochim. Acta, Part A*, **28**, 29 (1972).
(73) B. H. Freeland, J. L. Hencher, D. G. Tuck, and J. G. Contreras, *Inorg. Chem.*, **15**, 2144 (1976).
(74) R. A. Carney, E. A. Piotrowski, A. G. Meister, J. H. Braun, and F. F. Cleveland, *J. Mol. Spectrosc.*, **7**, 209 (1961).
(75) D. W. H. Rankin and A. Robertson, *J. Mol. Struct.*, **27**, 438 (1975); H. Oberhammer, *ibid.*, **31**, 237 (1976).
(76) S. Martinez, S. Garcia-Blanco, and L. Rivoir, *Acta Crystallogr.*, **9**, 145 (1956); J. A. Rausell-Colom and S. Garcia-Blanco, *ibid.*, **21**, 672 (1966); R. J. Guttormson and E. Stanley, *ibid., Sect. B*, **25** 971 (1969); R. N. Hargreaves and E. Stanely, *Z. Kristallogr., Kristallgeom., Kristallphys.*, **135**, 399 (1972).
(77) M. Bodenstein, P. Harteck, and E. Padelt, *Z. Anorg. Allg. Chem.*, **147**, 233 (1925).
(78) C. J. Schack and K. O. Christe, *Inorg. Chem.*, **13**, 2378 (1974).
(79) A. S. Parkes and R. E. Hughes, *Acta Crystallogr.*, **16**, 734 (1963).
(80) M. G. Inghram, R. F. Porter, and W. A. Chupka, *J. Chem. Phys.*, **25**, 498(1956).
(81) K. M. Maloney, S. K. Gupta, and D. A. Lynch, Jr., *J. Inorg. Nucl. Chem.*, **38**, 49 (1976).
(82) R. H. Jackson, *J. Chem. Soc.*, 4585 (1962).
(83) R. L. Kuczkowski, *J. Am. Chem. Soc.*, **86**, 3617 (1964).
(84) B. Beagley, G. H. Eckersley, D. P. Brown, and D. Tomlinson, *Trans. Faraday Soc.*, **65** 2300 (1969).
(85) E. Hirota, *Bull. Chem. Soc. Jpn.*, **31**, 130 (1958).
(86) S. G. Frankiss, *J. Mol. Struct.*, **2**, 271 (1968).
(87) G. Krummel and R. Minkwitz, *Inorg. Nucl. Chem. Lett.*, **13**, 213 (1977).
(88) B. M. Gimarc, *J. Am. Chem. Soc.*, **92**, 266 (1970).
(89) A. D. Kirshenbaum, A. V. Grosse, and J. G. Aston, *J. Am. Chem. Soc.*, **81**, 6398 (1959).
(90) M. M. Rochkind and G. C. Pimentel, *J. Chem. Phys.*, **46**, 448 (1967); W. G. Alcock and G. C. Pimentel, *ibid.*, **48**, 2373 (1968); F. K. Chi and L. Andrews, *J. Phys. Chem.*, **77**, 3062 (1973).
(91) R. J. Gillespie, J. B. Milne, and M. J. Morton, *Inorg. Chem.*, **7**, 2221 (1968).
(92) W. Giggenbach, *J. Inorg. Nucl. Chem.*, **30**, 3189 (1968).
(93) S. C. Abrahams, *Acta Crystallogr.*, **7**, 423 (1954).
(94) D. D. Davis and H. Okabe, *J. Chem. Phys.*, **49**, 5526 (1968); M. W. Slack, E. S. Fishburne, and A. R. Johnson, *ibid.*, **54**, 1652 (1971).
(95) D. White, D. E. Mann, P. N. Walsh, and A. Sommer, *J. Chem. Phys.*, **32**, 481 (1960).
(96) S. Smoes, C. E. Myers, and J. Drowart, *Chem. Phys. Lett.*, **8**, 10 (1971).
(97) J. Drowart, R. P. Burns, G. DeMaria, and M. G. Inghram, *J. Chem. Phys.*, **31**, 1131 (1959).
(98) K. S. Pitzer and E. Clementi, *J. Am. Chem. Soc.*, **81**, 4477 (1959).
(99) R. D. Brown and R. D. Harcourt, *Proc. Chem. Soc., London*, 216 (1961); *Aust. J. Chem.*, **16**, 737 (1963).
(100) R. D. Harcourt, *Theor. Chim. Acta*, **2**, 437 (1964); **3**, 19 (1965); **6**, 131 (1966); *J. Mol. Struct.*, **9**, 221 (1971).
(101) E. B. Moore, Jr., *Theor. Chim. Acta*, **7**, 144 (1967).
(102) T. F. Redmond and B. B. Wayland, *J. Phys. Chem.*, **72**, 3038 (1968).
(103) NOTE ADDED IN PROOF. Recent electron diffraction results show that B_2F_4 is planar: D. D. Danielson, J. V. Patton, and K. Hedberg, *J. Am. Chem. Soc.*, **99**, 6484 (1977).